

Krzysztof ZAK¹

INFLUENCE OF GRINDING CONDITIONS ON THE TOPOGRAPHIC CHARACTERISTIC OF MACHINED SURFACES

This paper compares the ability of grinding processes to enhance functional properties of the surface textures produced. The main objective of such a comparison is to facilitate the decision about precision grinding operations. The experimental study performed includes two grinding operations using electro-corundum Al_2O_3 and CBN wheels. For this purpose, the topographic features of ground surfaces with the S_a roughness parameter of about $0.2\ \mu\text{m}$ were compared. Apart from the set of 3D roughness parameters, the frequency, fractal, wavelet and motif characteristics were analyzed.

1. INTRODUCTION

Grinding and turning using CBN-based materials are largely employed in industry for the precision and high precision machining of hardened steels (45-60HRC) although conventional grinding operations using Al_2O_3 wheels are also employed due to their convenient cost which compensates a higher machining time and less productivity. Moreover, thermal damage of the surface layer is a common productivity limitation factor for conventional grinding. The application of super-abrasive technology limits the undesired thermal effects and enhances the surface quality and integrity of the machined parts. The main advantages of hard machining over grinding are high flexibility, possible complete machining, a lesser ecological burden and higher productivity (MRR) [1],[2]. However, its industrial potential is still limited due to the unsatisfactory surface integrity and the attainable dimensional and shape accuracy [1],[3]. As mentioned above special interest is focused on precision and high-precision machining operations which demand the R_z roughness parameter to be at $2.5\text{--}4\ \mu\text{m}$ and below $1\ \mu\text{m}$ respectively [4]. Moreover, it is important to investigate the capabilities of all applicable operations to the functionality of the machined surfaces [5]. In this aspect, a special attention is focussed on the comprehensive characterization of surface finish and surface texture produced by these challenging operations [5],[6]. This is because they generate different surface structures

¹ Opole University of Technology, Faculty of Mechanical Engineering, Poland,
E-mail: k.zak@po.opole.pl

which influence various functional properties, predominantly the fatigue strength and wear resistance.

Because surface functionality depends on the surface geometrical structure, the topographical (3D) analysis should be performed.

Nowadays, the technological shifts in surface metrology allow the surface features generated by modern manufacturing processes (including machining of hardened steels) to be characterized with a higher accuracy using a number of the field parameters (S-parameters and V-parameters sets) [7]. Special visualization tools in this area have been developed allowing a more comprehensive characterization of the machined surfaces [7],[8],[9]. This paper presents the results of a comparative investigation of surfaces generated during the cylindrical grinding using Al_2O_3 and CBN wheels. In particular, surface textures of differently ground surfaces with the Sa parameter of about $0.2\mu m$ are characterized and compared using a number of standardized 3D roughness parameters as well as motif and frequency parameters.

2. EXPERIMENTAL PROCEDURE

2.1. MACHINING CONDITIONS

This experimental study includes precision hard turning and grinding operations on samples made of a 41Cr4 (AISI 5140 equivalent) steel with Rockwell's hardness of 57 ± 1 HRC and initial Sa roughness of about $0.4\mu m$. Turning was performed using CBN tools (grade CB7015 by Sandvik Coromant) with cutting parameters permitting the Sa roughness of about $0.45\mu m$. TNGA 160408 S01030 chamfered inserts with brazed-CBN tips were used. The machine tool was a CNC turning center, Okuma Genos L200E-M. Grinding operations were performed on conventional cylindrical grinding machines using electro-corundum Al_2O_3 and CBN wheels and a water soluble emulsion as a coolant. Similarly, surfaces with the Sa near $0.2\mu m$ were produced. Machining conditions for two turning and two abrasive operations are specified in Table 1.

Table 1. Initial hard turning and precision cylindrical grinding conditions

Symbol	Machining operation	Machining conditions
HT (INIT)	Hard turning using CBN TNGA 160408 S01030 chamfered insert	$v_c=150\text{m/min}$, $f=0.1\text{mm/rev}$, $a_p=0.15\text{mm}$
GR1	Cylindrical grinding using Al_2O_3 ceramic, $350\times 25\times 127$ 32A grinding wheel	$v_c=11.9\text{ m/s}$, $a_e=0.025\text{mm}$, $f_a=3.5\text{mm/rev}$
GR2	Cylindrical grinding using INTER DIAMENT B107 K100 SV grinding wheel	$v_c=36\text{ m/s}$, $a_e=0.025\text{mm}$, $f_a=1.6\text{ mm/rev}$

2.2. CHARACTERIZATION OF SURFACE ROUGHNESS AND TEXTURE

In this study, surface topographies generated by CBN tools and Al_2O_3 and CBN wheels were measured by means of the stylus method using a TOPO-01P contact profilometer with a diamond stylus radius of $2\pm 0.5\mu\text{m}$. 3D roughness parameters were determined and surface topographies were visualized using a Digital Surf, Mountains® Map package. They include: a) standardized five subgroups of 2D and 3D surface roughness parameters: height, amplitude, horizontal, hybrid and functional, b) standardized motif parameters, c) characteristics of frequency spectra recorded.

3. EXPERIMENTAL RESULTS AND DISCUSSION

3.1. CHARACTERIZATION OF SURFACE PROFILE AND TOPOGRAPHY

Representative surface profiles obtained in hard turning and grinding operations along with the values of roughness parameters are presented in Figs. 1a-b. Grinding produced profiles (Figs. 1a and b) with densely distributed irregularities (smaller R_{sm} value) and higher slopes ($R_{\Delta q}\approx 3-4^\circ$) in comparison to CBN hard turning with the feed rate of 0.06mm/rev . As shown in Fig. 1, the grinding of the hard turned surface causes that regular (deterministic) surface lays generated by hard turning become partly random (Fig. 1a and b). Moreover, deep notches appearing in ground profiles can adversely influence fatigue strength.

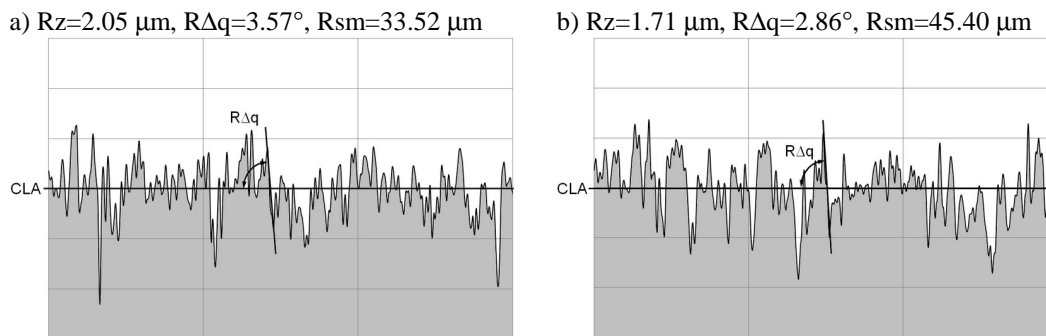


Fig. 1. Modifications of initial turned surface profile by precision grinding using electro-corundum (a) and CBN (b) wheels

Representative surface topographies obtained in hard turning and grinding operations performed are presented in Figs. 2a–b. From the practical point of view, the comparison of the S_a and S_z roughness parameters which are frequently used by constructors and technologists is of fundamental importance. In terms of the surface quality criterion discussed in the introduction both operations can be classified as precision machining,

although hard turning is close to high-precision machining for which Rz parameter should be less than $1\mu\text{m}$ (the measured Rz is equal to $1.25\mu\text{m}$).

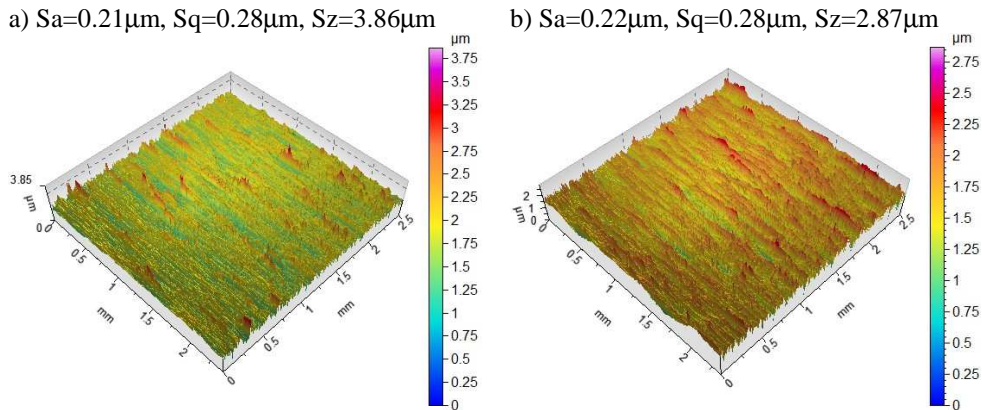


Fig. 2. Surface textures produced by grinding using ceramic (a) and CBN (b) wheels

The measured values of S_a and S_z parameters are equal $0.21\mu\text{m}$ and $3(4)\mu\text{m}$ for grinding with different wheels. It should be noted that values of R_z are substantially lower than S_z for grinding – for surfaces ground with Al_2O_3 wheels $R_z=2.4\mu\text{m}$ and $S_z=3.9\mu\text{m}$. This comparison clearly depicts that ground surfaces contain a number of high sharp peaks which distinctly increase the total height S_z , in this case study up to $4\mu\text{m}$, although the S_a parameter is equal to about $0.2\mu\text{m}$.

It can be observed in Fig. 2 that the ground surfaces are random anisotropic but zoomed isometric views suggest the presence of periodic components. The strong anisotropy of all surfaces shown in Fig. 2 is confirmed by characteristic shapes of the autocorrelation function (AACF) presented in Fig. 3.

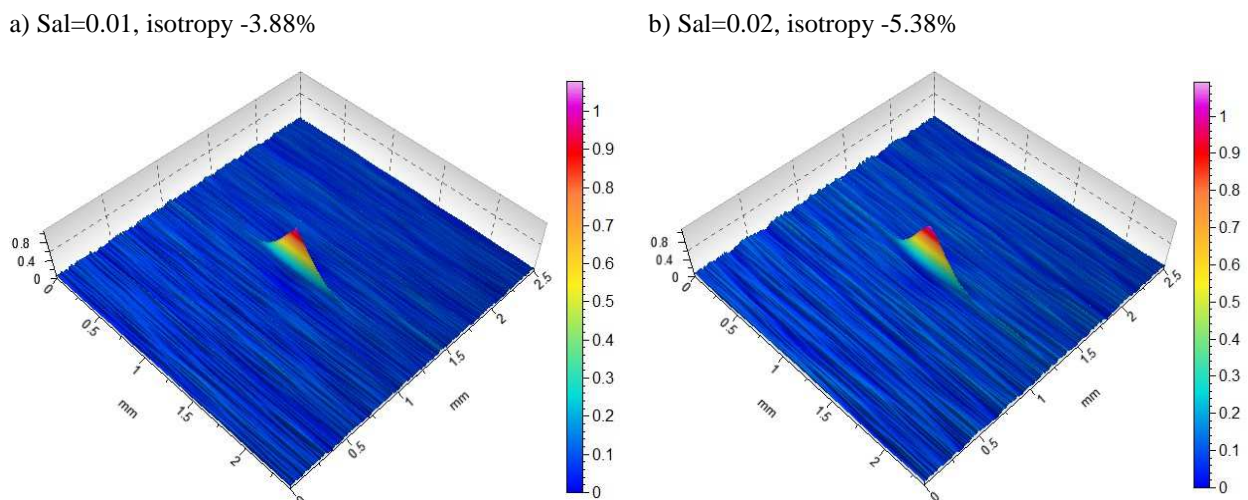


Fig. 3. Representative autocorrelation functions for ground surfaces using Al_2O_3 (a) and CBN (b) wheels

From this point of view, the ground surface is mixed, between anisotropic and random structures. In both cases (Figs. 3a and b) an exponential function with a characteristic decay of the periodicity is depicted. Moreover, the content of isotropy in the ground surfaces is not higher than 6% (higher for CBN ground surface). The values of the fastest decay autocorrelation length (S_{al}) are equal to 0.01 and 0.02 for cases a and b respectively. A low S_{al} values for the ground surfaces indicate that high spatial frequency components are dominated (see Figs. 9a and b).

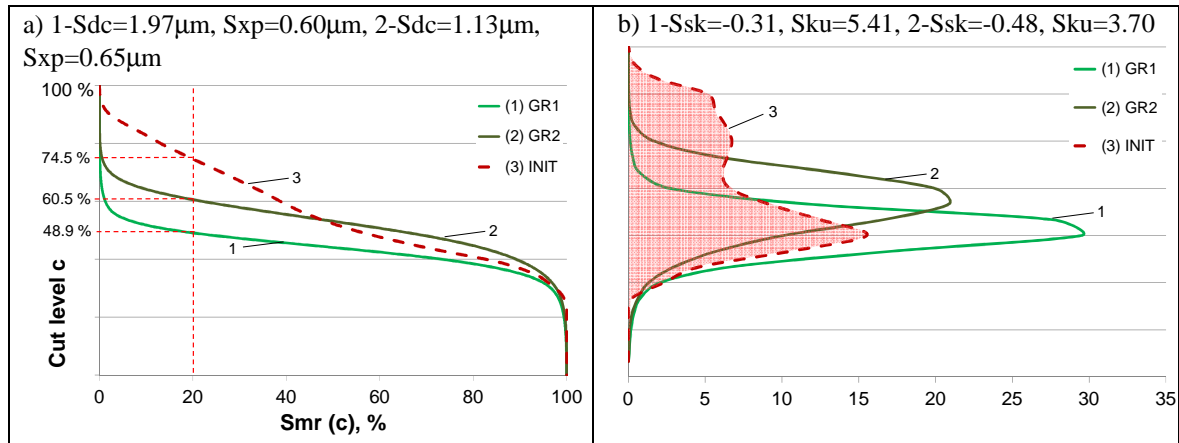


Fig. 4. 3D BAC shapes: (a) and ADF distributions, (b) for ground (curves 1 and 2) surfaces

3.2. CHARACTERIZATION OF AREA BEARING PROPERTIES

Fig. 4 presents the 3D bearing area curves (3D BAC) and associated ADF curves obtained for the compared surfaces. Finish grinding generates surfaces with S-shape BAC (1 and 2) and negative skewness S_{sk} . It is worth noticing that the values of S_{sk} for both ground surfaces differ visibly- (-0.31 for GR1) versus (-0.48 for GR2). It can be seen in Fig. 4b that two precision processes (GR1 and GR2) produce non-Gaussian distributions of surface heights but ADF shapes are different for ground topographies. Also using Al_2O_3 and CBN wheels results in various bearing properties of ground surfaces. As a result, there is a flexibility in changing the initial ADF curve (3) by subsequent grinding passes.

An additional characterization of 3D BAC presented in Fig. 4a is provided by the areal material ratio $S_{mr}(c)$, the inverse areal material ratio $S_{dc}(mr)$ and the peak extreme height S_{xp} . Relevant values of these parameters for three machined surfaces are specified in Fig. 4a.

Trends in modification of 3D bearing parameters (S_{pk} , S_k , S_{vk}) caused by precision grinding are illustrated in Fig. 6. The first finding is that the values of the reduced peak height S_{pk} decrease from about $0.6\mu m$ to $0.2-0.25\mu m$ and the wear resistance of both ground surfaces is comparable. Moreover, the exploitation allowance defined by the core distance is also comparable- $S_k = 0.6-0.7\mu m$. In contrast, the reduced valley height S_{vk} for ground surfaces is distinctly higher than the reduced peak height.

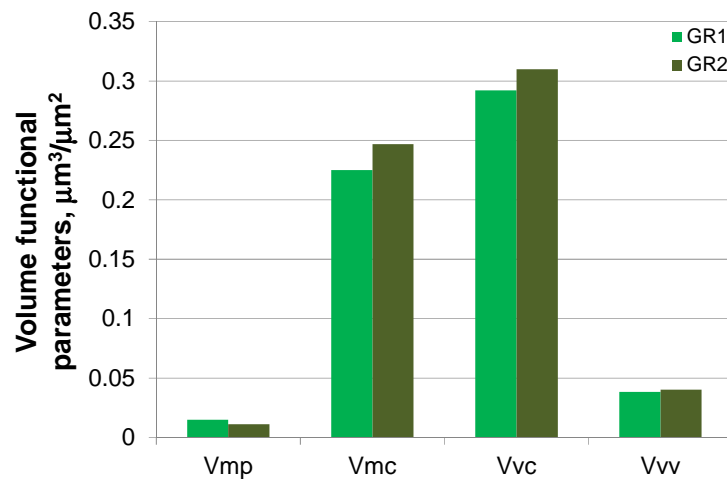


Fig. 5. Distribution of volume functional parameters for ground surfaces. GR1 - ($V_{mp}=0.0150\mu\text{m}^3/\mu\text{m}^2$, $V_{vc}=0.292\mu\text{m}^3/\mu\text{m}^2$, $V_{mc}=0.225\mu\text{m}^3/\mu\text{m}^2$, $V_{vv}=0.0383\mu\text{m}^3/\mu\text{m}^2$); GR2 - ($V_{mp}=0.0112\mu\text{m}^3/\mu\text{m}^2$, $V_{vc}=0.310\mu\text{m}^3/\mu\text{m}^2$, $V_{mc}=0.247\mu\text{m}^3/\mu\text{m}^2$, $V_{vv}=0.0403\mu\text{m}^3/\mu\text{m}^2$)

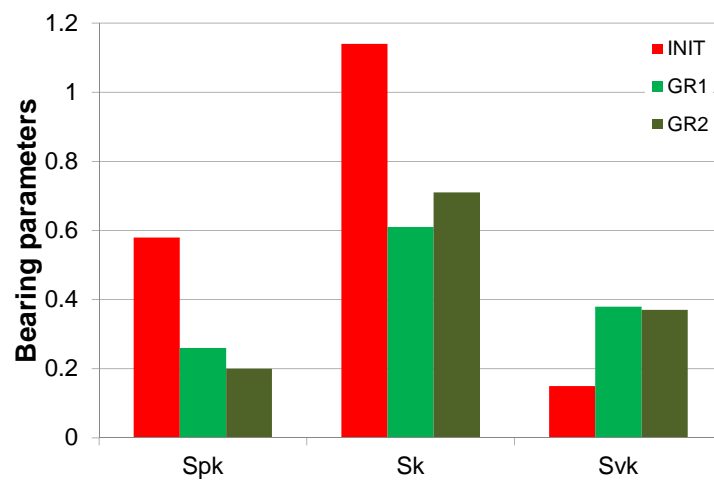
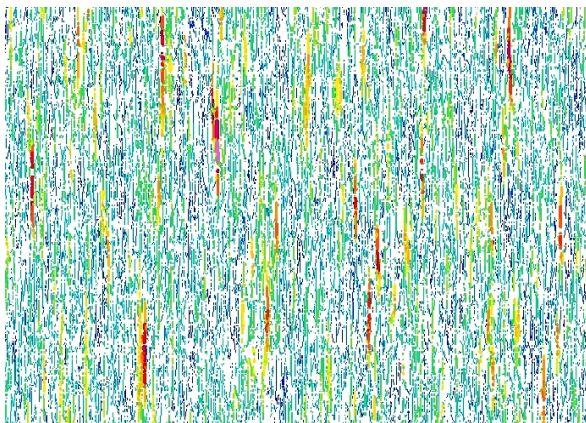
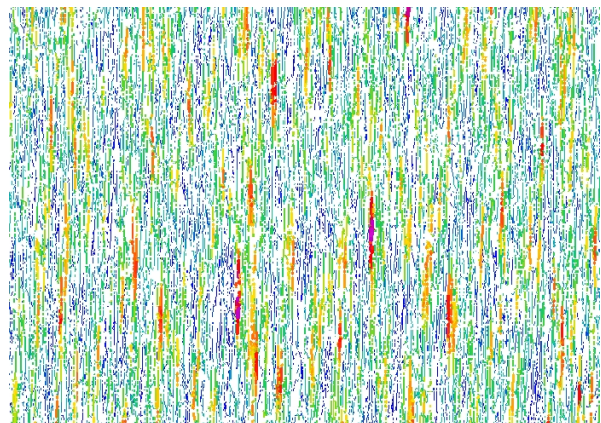


Fig. 6. Distribution of areal bearing parameters for ground surfaces

a1) $1.97\mu\text{m}/0.45\mu\text{m}/709\text{cm}/\text{cm}^2$



b1) $1.76\mu\text{m}/0.46\mu\text{m}/708\text{cm}/\text{cm}^2$



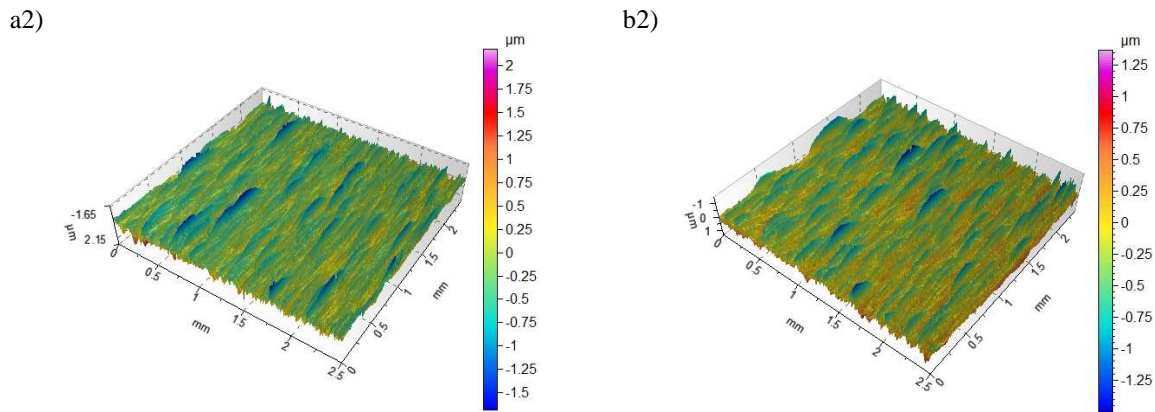


Fig. 7. Vectorized micro-valleys networks (a1 and b1) and isometric views of valleys (a2 and b2) for ground surfaces using Al_2O_3 (a) and CBN (b) wheels. Three values describe the average depth, width and density of micro-valleys

Additional information on the fluid retention between the matting surfaces can be obtained using an original technique of the vectorisation of micro-valleys network generated on the machined surface [8],[9]. On the other hand, isometric views of valleys are presented in Figs. 7a2 and b2. Such visualizations allow the deep notch to be precisely selected. Characteristic nets of micro-grooves visualized for ground surfaces are illustrated in Fig. 7. The maximum depth of valleys is about $2\mu\text{m}$ and their widths are equal to $0.5\mu\text{m}$. By grinding, the average density of valleys increases to above $700\text{cm}/\text{cm}^2$. These data coincides well with the distributions of the volume functional parameter (V_{mp} and V_{vv}) shown in Fig. 5. Moreover, vectorial images shown in Fig. 7 confirm that the generated surfaces are mixed periodic-random anisotropic.

The functional topographical features of the machined surfaces can be assessed by means of the volume parameters including the peak material volume (V_{mp}), the core material volume (V_{mc}), the core void volume (V_{vc}) and the valley void volume (V_{vv}) parameters. [10],[11]. Their values measured for turned and ground topographies are equal to (in order GR1/GR2): $V_{\text{mp}}=0.0150/0.0112\mu\text{m}^3/\mu\text{m}^2$; $V_{\text{mc}}=0.225/0.247\mu\text{m}^3/\mu\text{m}^2$; $V_{\text{vc}}=0.292/0.310\mu\text{m}^3/\mu\text{m}^2$; $V_{\text{vv}}=0.0383/0.0403\mu\text{m}^3/\mu\text{m}^2$. In particular, a better fluid retention ability of ground surfaces is associated with relatively higher values of $V_{\text{vv}}=0.0385$ and $0.0403\mu\text{m}^3/\mu\text{m}^2$.

3.3. AREA SPATIAL AND HYBRID PARAMETERS

The 12 S-parameter set includes four spatial parameters- the density of summits S_{ds} , the autocorrelation length (the fastest decay autocorrelation length) S_{al} , the texture aspect ratio S_{tr} , the texture direction S_{td} , three of which are texture parameters (S_{al} , S_{tr} and S_{td}). The ground surfaces contain distinctly more summits within the scanned area - $S_{\text{ds}}=1305.6$ $1/\text{mm}^2$ versus 1123.9 $1/\text{mm}^2$ for turned surfaces. The comparable small texture aspect ratio $S_{\text{tr}}=0.04-0.07$ for ground surfaces indicates stronger directionality (anisotropy). In general, S_{tr} values less than 0.1 are characteristic for highly anisotropic surfaces [10]. The texture

direction Std close to 90° for machined surfaces indicates that the dominant surface lay is perpendicular to the measurement direction. The values of Sal parameter obtained (0.02mm vs. 0.01mm) suggest that the ground texture is dominated by short wavelength patterns. This conclusion agrees with the APS spectra shown in Fig. 9.

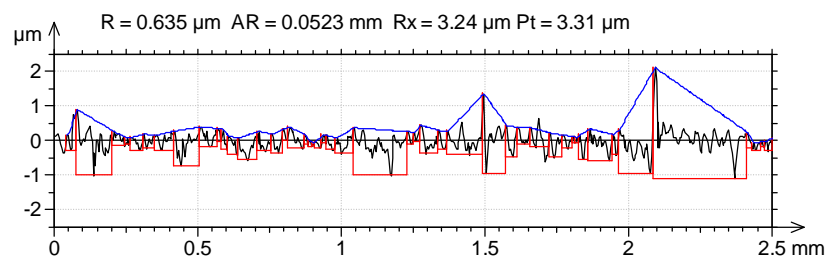
The 3D hybrid parameters are: the RMS slope Sdq, the developed interfacial area ratio Sdr and the average summit curvature Ssc. The ground surfaces contain irregularities with slopes Sdq of about 60 and this trend coincides qualitatively with 2D slope data. The value of the Ssc of about $0.02\mu\text{m}^{-1}$ for the ground surfaces agrees with those for typical machined surfaces ($0.004\text{-}0.03\mu\text{m}^{-1}$) given in [10]. The Sdr parameter is higher for ground surfaces (Fig. 2a and b) for which the smallest unit of plane area is about 0.16 %.

3.4. MOTIFS

The motif analysis is performed on the unfiltered surface profile divided into a series of windows [9], as shown in Fig. 9. The roughness motifs marked by the segment frames are characterized by the mean depth R, the mean spacing AR and the largest motif height Rx. The comparison of motif parameters specified in Fig. 8 indicates that ground surfaces include distinctly deeper pits ($R_x=1.68$ and $2.55\mu\text{m}$) which is in accordance with the surface topographies shown in Fig. 2 and volume bearing parameters shown in Fig. 5. The distribution of motif windows for the ground surface confirms enhanced fluid retention in comparison to the turned surface with a comparable Sa value [12].

It is clear in Fig. 9 that the Rx motif parameter is stronger correlated with the Sz parameter rather than Rz although motifs are based on 2D analysis. On the other hand, the R motif parameter of $0.6\text{-}0.7\mu\text{m}$ seems to be independent of the grinding conditions used.

a) GR1



b) GR2

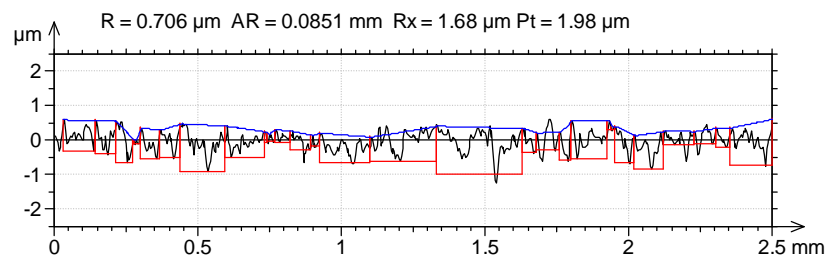


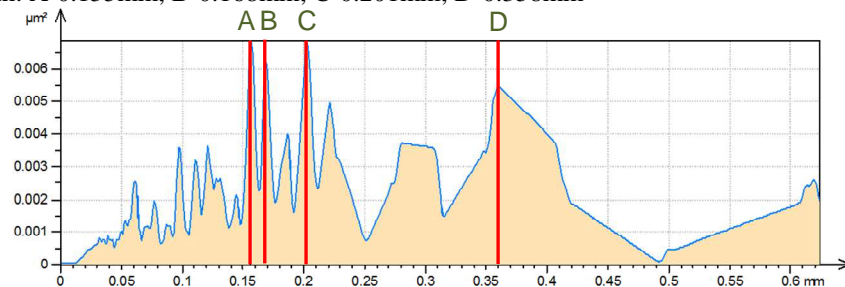
Fig. 8. Motif graphs for ground surfaces using Al_2O_3 , (a) and CBN, (b) wheels

3.5. FREQUENCY ANALYSIS

The Power Spectral Density (PSD) is very sensitive for all disturbances of the generated surfaces which appear in the technological machining system. The PSD spectra obtained for hard turned and ground surfaces are presented in Fig. 9.

It is evident in Fig. 9 that both ground surfaces (Fig. 9a and b) are generated with the presence of machining vibrations and the PSD spectrum contains several components with longer wavelengths –the first one of about 0.15mm in length for both grinding operations, and slightly lower amplitudes of 0.06-0.08 μm for shorter wavelengths.

- a) GR1; Amplitude: A-0.0829 μm ; B-0.0772 μm ; C-0.0826 μm ; D-0.074 μm
Wavelength: A-0.155mm; B-0.168mm; C-0.201mm; D-0.358mm



- b) GR2; Amplitude: A-0.0677 μm ; B-0.0741 μm ; C-0.0629 μm ; D-0.105 μm
Wavelength: A-0.148mm; B-0.185mm; C-0.223mm; D-0.316mm

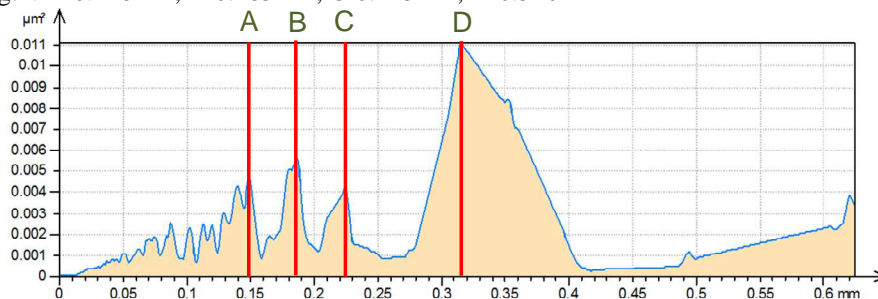


Fig. 9. Averaged power spectral density(PSD) for ground surfaces using Al₂O₃ (a) and CBN (b) wheels

In particular, smaller amplitudes were recorded in the middle of the PSD spectrum for surfaces produced by grinding using CBN wheel (Fig. 9a) rather than ceramic wheel (Fig. 9b). This fact suggest that grinding with a CBN wheel was relatively stable.

4. CONCLUSIONS

1. It was documented that topographic features of ground surfaces with the same Sa parameter of about 0.2 μm are different. This fact suggests that their functional properties should also be different.

2. The textures of ground surfaces are mixed periodic–random anisotropic respectively. This difference can be determined based on 3D surface topographies, the distributions of the PSD function as well as vectorial maps of micro-valleys. However, the disturbances of regular surface structures by grinding can result from both the kinematical and tribological effects.
3. 3D BAC curves and appropriate functional parameters depict that ground hard surfaces have better fluid retention abilities. This is due to higher negative Ssk value and higher Vvv volumes for ground textures. It was also documented, based on vectorial maps of micro-valleys, by deeper and wider grooves as well as higher average density of valleys.
4. Al₂O₃ and CBN ground textures have similar tribological properties because of comparable Vmp and Spk parameters, which suggest practically the same material allowance to be removed during running-in period.

REFERENCES

- [1] KÖNING W., BERKTOLD A., KOCH K.F., 1993, *Turning versus grinding- a comparison of surface integrity aspects and attainable accuracies*. CIRP Annals, 42/1, 39-43.
- [2] DAVIM J.P. (ed.), 2011, *Machining of hard material*, Springer, London.
- [3] BARTARYA G., CHOUDHURY S.K., 2012, *State of the art in hard turning*, Int. J. Mach. Tools Manuf., 53, 1-14.
- [4] KLOCKE F., 2011, *Manufacturing processes I. Cutting*, Springer-Verlag, Berlin.
- [5] WAIKAR R.A., GUO Y.B., 2008, *A comprehensive characterization of 3D surface topography induced by hard turning versus grinding*, J. Mat. Proc. Technol., 197, 189-199.
- [6] GRZESIK W., RECH J., WANAT T., 2007, *Surface finish on hardened bearing steel parts produced by superhard and abrasive tools*, Int. J Mach Tools Manuf., 47, 255-262.
- [7] JIANG X.J., WHITEHOUSE D.J., 2012, *Technological shifts in surface metrology*, CIRP Annals, 61/2, 815-836.
- [8] LONARDO P.M., TRUMPOLD H., DE CHIFFRE L., 1996, *Progress in 3D surface microtopography characterization*, CIRP Annals, 45/2, 589-598.
- [9] DE CHIFFRE L., LONARDO P.M., TRUMPOLD H., et al., 2000, *Quantitative characterization of surface texture*, CIRP Annals, 49/2, 635-652.
- [10] GRIFFITHS B., 2001, *Manufacturing surface technology. Surface integrity and functional performance*, Penton Press, London.
- [11] LEACH R. (ed.), 2013, *Characterization of areal surface texture*. Springer-Verlag, Berlin.
- [12] GRZESIK W., ZAK K., 2013, *Comparison of surface textures produced by finish cutting, abrasive and burnishing operations in terms of their functional properties*, J. Mach. Eng., 13/2, 46-58.